

Molecular quantum wave-packet splitting and revivals in shared phase space

Dong Wang, Åsa Larson, and Tony Hansson*

Stockholm University, Department of Physics, AlbaNova University Center, SE-106 91 Stockholm, Sweden

Hans O. Karlsson

Uppsala University, Department of Physical and Analytical Chemistry, Quantum Chemistry, Box 518, SE-751 20 Uppsala, Sweden

(Received 24 September 2008; published 2 February 2009)

The evolution of a molecular wave packet created by an ultrashort laser pulse in a system of two coupled bound states is investigated by quantum dynamics calculations and semiclassical theory. Under suitable dynamical quantum interference conditions, the wave packet may be split into two separable fractions that move in different but partially overlapping regions of the energetically available phase space. Each wave-packet part can be individually addressed in the divided parts of the molecular phase space, and they are shown to go through separate long-term collapse-revival cycles analogous to those of wave packets moving in single anharmonic potentials. In a pump-probe scheme, the dynamics of the system would look very different depending on what internuclear distances are probed. The regular dynamics observable in the separated parts of the phase space takes on a quite irregular appearance in the regions that are shared by the wave-packet components. The wave-packet regularity is shown to depend sensitively on the pump pulse wavelength, which is a reflection of the energy range over which the quantum interference conditions are maintained. These conditions, as well as the wave-packet fraction revival times, are well reproduced by semiclassical theory.

DOI: [10.1103/PhysRevA.79.023402](https://doi.org/10.1103/PhysRevA.79.023402)

PACS number(s): 42.50.Md, 82.53.Hn, 82.50.Nd, 82.20.Gk

I. INTRODUCTION

Interference of matter waves is a genuine quantum effect without correspondence in our classical-appearing world of everyday life. With the recent realization of macroscopic coherent ensembles of atoms, however, the avenue to practical applications like quantum computers has been laid open, with immense potential implications for society. This has led to a rapidly increasing interest in searching and exploring schemes for quantum manipulation of matter like molecules [1,2].

Quantum interference effects on matter dynamics is a concept as old as quantum mechanics itself [3]. In the molecular physics framework of the present article, it was shown in early work by Stückelberg [4] that interference at an intersection of two electronic potential energy curves could cause the electronic excitation probability in atomic collisions to oscillate with collision energy. Later on, such interference was invoked to explain unexpectedly long-lived rovibronic states in predissociative systems [5]. The quantum wave-packet viewpoint, however, laid dormant more or less until the advent and implementation of femtosecond lasers some 20 years ago. The analysis of the first experiment on a predissociative molecular system [6] made clear that quantum wave-packet interference played a decisive role in the molecular break up [7–9].

Interference is most pronounced in systems with strong coupling—that is, where the dynamics comprises maximally mixed diabatic and adiabatic evolution. Recent experiments on predissociative molecular systems in this coupling range [10], indeed, bear strong traits of quantum interference [11,12]. In the same vein, we showed [13–15] that also systems consisting of two strongly coupled bound molecular

states exhibit quantum interference effects of the same kind. In that case, however, the dynamics is richer. The single combination of interfering hybrid diabatic-adiabatic wave-packet paths in unbound systems is in bound systems replaced with four principle combinations of two kinds—*mesobatic bistable* and *mesobatic astable* [13,14] (see the following section for definitions)—depending on the initial conditions. There is no fundamental reason why these phenomena should be restricted to molecular systems and, indeed, we recently showed that they appear also in models of standing-wave laser-driven harmonically trapped ions [16].

The interesting idea to enhance the quantum interference effect by adjustment of the involved potential energy curves was shown by Dietz and Engel [17] to be very potent on the time scale of molecular vibrations. We used the same approach to show that interference has profound implications also on the normally much longer time scale of molecular wave-packet revivals [18]. In fact, under optimized conditions wave packets that are moving in maximally coupled systems undergo collapse-revival cycles with fractional and full revivals exactly analogous to those of a wave packet moving in a single anharmonic potential. The revival time, however, is modified to be intermediate to those of the active diabatic and adiabatic pathways, respectively, in proportion to the wave-packet splitting at the crossing of the potential curves [18].

In the present article we extend the previous work on two-state systems to a three-state model based on the lowest electronic states of Rb_2 (see Fig. 1), including a wave-packet preparation stage by ultrafast laser excitation from the ground state. The system parameters are varied in order to identify optimal conditions for quantum interference in the coupled excited states. The characteristic dynamical features of the optimized system are analyzed within a semiclassical framework, and the potential of using the laser wavelength to tune the wave-packet conditions is examined. Under optimal wave-packet conditions, the ensuing dynamics is shown to

*tony.hansson@physto.se

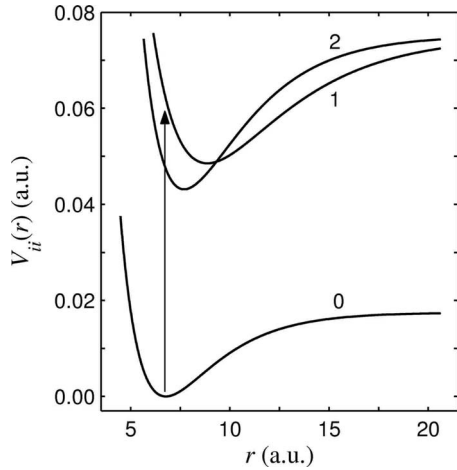


FIG. 1. Model molecular system. Electronic states are labeled numerically, and lines are the corresponding (diabatic) potential energy curves as a function of internuclear separation r . The states $|1\rangle$ and $|2\rangle$ are coupled by a Gaussian function of r , and an ultrashort laser pulse couples the initial wave packet in $|0\rangle$ to $|1\rangle$ (vertical arrow). See Sec. III for specifications.

comprise the formation of two wave-packet fractions with independent long-term collapse-revival dynamics. The signature of this state of motion, moreover, is shown to be strongly dependent on the choice of probe point. From a coherent control perspective, we here present a scheme for persistent splitting of a wave packet moving in a system of two strongly coupled bound states.

II. REGULAR HYBRID WAVE-PACKET MOTION AND SEMICLASSICAL THEORY

The regular hybrid diabatic-adiabatic wave-packet motion that results from fulfilment of the requirements for complete quantum interference can be understood in good detail from semiclassical arguments [13,14,18]. In this section we illustrate the basic types of regular hybrid dynamics that appears and introduce some simplifying nomenclature [13,14]. Semiclassical interference conditions for each hybrid motion type are reviewed as well as the corresponding revival times [18]. In Sec. IV we will find use of these results to interpret the more involved wave-packet dynamics in the present system.

A. Types of regular hybrid motion

The system of two strongly coupled excited states in Fig. 1 can support two basic types of regular hybrid diabatic-adiabatic wave-packet motion. To reduce cluttering of the language, we will in the following use the more concise phrase *mesobatic* motion to denote generically these two kinds of regular wave-packet motion.

In the first type of mesobatic motion, which also occurs in predissociative systems and there gives rise to long-lived resonances, the wave-packet $|\Psi;t\rangle$ starts out in one diabatic state, splits at the potential curve crossing, and after turning around recombines at the crossing to the same diabatic state as the initial one. This behavior is visualized through the

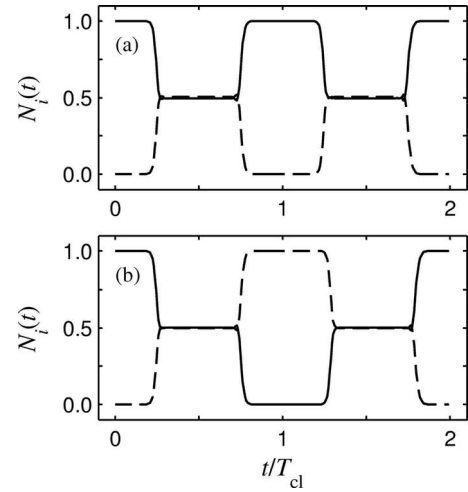


FIG. 2. Time-dependent populations $N_i(t) = \langle \Psi;t|i\rangle\langle i|\Psi;t\rangle$ of the two diabatic states $i=1$ (solid lines) and 2 (dashed line) under mesobatic interference conditions. In both panels the normalized wave packet, $N_1(t)+N_2(t)=1$, starts out being well localized at a turning point in $|1\rangle$. T_{cl} is the average classical vibrational period of the initial diabatic state. Cases: (a) bistable (b) astable.

time-dependent populations of the diabatic states, $N_i(t) = \langle \Psi;t|i\rangle\langle i|\Psi;t\rangle$, in Fig. 2(a). There is a companion state of motion which differs to the previous one only in that it starts out in the other diabatic state on the same side of the potential curve crossing. These two states of motions we call *bistable* in analogy with an electronic flip-flop switch that can be set to and remain in either one of two states. Notably, this type of motion can occur for any value of the wave-packet splitting ratio at the first encounter of the potential curve crossing.

The other kind of basic mesobatic wave-packet motion, similarly illustrated in Fig. 2(b), may appear with a slight shift in wave-packet energy or system parameters from the bistable situation. In this *astable* state the wave packet always recombines to the diabatic state opposite to the one it came from before splitting at the potential curve crossing. Thus, the recombined wave packet will undergo a kind of regular oscillation in appearance at the outer turning points of the diabatic states, similar to an electronic switch that can be set to oscillate between its two states. The astable state for obvious reasons cannot occur in predissociative systems. Moreover, to be effective it requires very nearly 50:50 wave-packet splitting at the first passage of the potential energy curve crossing, *vide infra*.

B. Mesobatic interference conditions

The interference conditions for the two basic types of mesobatic wave-packet motion are readily obtained in the framework of semiclassical wave-packet dynamics [7,14,17]. For this we presume that the in- and outward curve crossing events for a well-localized wave packet are described by the matrices [19]

$$T_{\times}^{\text{in}} = \begin{bmatrix} \sqrt{1-f}e^{ix} & \sqrt{f} \\ -\sqrt{f} & \sqrt{1-f}e^{-ix} \end{bmatrix}, \quad (1)$$

$$T_{\times}^{\text{out}} = \begin{bmatrix} \sqrt{1-f}e^{i\chi} & -\sqrt{f} \\ \sqrt{f} & \sqrt{1-f}e^{-i\chi} \end{bmatrix}, \quad (2)$$

and the inner and outer parts of the wave-packet propagation including turnaround are described by [19]

$$P^{\text{in}} = \begin{bmatrix} e^{2i(\alpha_+-\pi/4)} & 0 \\ 0 & e^{2i(\alpha_--\pi/4)} \end{bmatrix}, \quad (3)$$

$$P^{\text{out}} = \begin{bmatrix} e^{2i(\beta_+-\pi/4)} & 0 \\ 0 & e^{2i(\beta_--\pi/4)} \end{bmatrix}. \quad (4)$$

In these matrices, f is the nonadiabatic transfer probability and χ is the relative phase arising from the crossing process, both of which are here calculated within the Landau-Zener approximation [19–21]. The α_{\pm} and β_{\pm} are accumulated phases due to propagation along parts of the adiabatic potential curves $V_+(r)$ (upper) and $V_-(r)$ (lower) of the corresponding coupled diabatic states $|1\rangle$ and $|2\rangle$. These phases are calculated in the WKB approximation as [19,22–24]

$$\alpha_{\pm} = \int_{\text{ITP}}^{r_{\times}} k_{\pm}(r)dr, \quad \beta_{\pm} = \int_{r_{\times}}^{\text{OTP}} k_{\pm}(r)dr. \quad (5)$$

ITP and OTP denote the pertinent inner and outer classical turning points, r_{\times} is the crossing point of the two diabatic potential curves, and $\hbar k_{\pm}(r) = \sqrt{2\mu[E - V_{\pm}(r)]}$ is the momentum of the reduced molecular mass μ at the total energy E . The overall matrix governing the evolution over a classical vibrational period for a wave packet that initially moves inwards then can be expressed as

$$M = P^{\text{out}}T_{\times}^{\text{out}}P^{\text{in}}T_{\times}^{\text{in}} = \begin{bmatrix} e^{2i\sigma_+}[(1 - e^{2i\delta})f - 1] & e^{2i(\sigma_+-\chi/2)}(e^{2i\delta} - 1)\bar{f} \\ e^{2i(\sigma_+-\chi/2)}(1 - e^{-2i\delta})\bar{f} & e^{2i\sigma_-}[(1 - e^{-2i\delta})f - 1] \end{bmatrix}, \quad (6)$$

where $\bar{f} = \sqrt{f(1-f)}$, $\sigma_{\pm} = \alpha_{\pm} + \beta_{\pm} \pm \chi$ is the total accumulated phase along a particular adiabatic path, and $\delta = \alpha_- - \alpha_+ - \chi$ is the accumulated phase difference for propagation in the inner parts of the two adiabatic potentials including the curve crossing.

Now, bistable motion requires M to be diagonal with conserved norm for the ingoing wave function. The only non-trivial condition for this to occur is $e^{2i|\delta|} = 1$, which is equivalent to

$$\delta = m\pi, \quad \text{integer } m. \quad (7)$$

Then

$$M_{\text{bistable}} = \begin{bmatrix} -e^{2i\sigma_+} & 0 \\ 0 & -e^{2i\sigma_-} \end{bmatrix}. \quad (8)$$

Under the bistable interference condition, thus, the initial wave packet is retained irrespective of its initial electronic state and the splitting ratio at the curve crossing. In other words, there are two coexisting basic bistable motions depending on the initial wave-packet state.

Astable mesobatic dynamics, on the other hand, results provided M is antidiagonal with preserved norm. From inspection of (6) we see that this requires that

$$\begin{cases} \delta = \left(m + \frac{1}{2}\right)\pi, & \text{integer } m, \\ f = \frac{1}{2} \end{cases} \quad (9)$$

which gives

$$M_{\text{astable}} = \begin{bmatrix} 0 & -e^{2i(\sigma_+-\chi/2)} \\ -e^{2i(\sigma_+-\chi/2)} & 0 \end{bmatrix}, \quad (10)$$

in accordance with the requirements. Again there are two coexisting motions depending on the initial electronic state. Different to the bistable case, however, the astable state of motion depends critically on the wave packet splitting into equally large fractions at the potential energy curve crossing.

C. Revival of bistable wave packets

A wave packet in a bistable state of motion undergoes long-term collapse-revival cycles fully analogous to those occurring for motion in single anharmonic potentials [18]. As such, the revival structures are signatures of quite regularly spaced energy levels in the coupled system and the revival period can be obtained by employing the same semiclassical formalism as the one used to deduce the mesobatic interference conditions (7) and (9) [18].

In the time-dependent semiclassical formulation of Chapman and Child [8], a predissociating wave packet comprises a superposition of eigenstates of the coupled system with complex eigenenergies and real amplitudes. A bistable state of wave-packet motion requires the whole range of eigenstates to be long lived, which may occur when a vibrational level v_d in the diabatic state is nearly degenerate with an adiabatic one v_a [5]—that is, when $E_d(\hat{v}_d) - E_a(\hat{v}_a) \approx 0$. Then, assuming that the quantum-state population is centered around the resonant pair \hat{v}_d and \hat{v}_a , the energy levels of the coupled system may be written in terms of a common quantum number $v = v_i - \hat{v}_i$ as

$$\bar{E}(v) = \frac{E_d(v) + x(v)E_a(v)}{1 + x(v)}, \quad (11)$$

where $x(v) = f\gamma(v)/(1-f)$ with $\gamma(v) = \omega_d(v)/\omega_a(v)$ and $\omega_i(v)$ denoting the local vibrational angular frequency in state i . Implicitly, also the nonadiabatic transfer probability f depends on v . Now, provided $\hat{v}_i \gg \Delta v \gg 1$, where Δv is the population distribution spread in v , $\bar{E}(v)$ can be expressed as a MacLaurin expansion in v from which the full revival period for the coupled system can be identified as [25]

$$T_{1/1}^{\text{rev}} = \frac{4\pi\hbar}{|\bar{E}''(v)|}. \quad (12)$$

Bistable motion requires the vibrational periods of the involved adiabatic and diabatic states to be equal; i.e., we have necessarily $\gamma(v) \approx 1$. Then, in the limit of exact resonance, $E_d(v) - E_a(v) \rightarrow 0$,

$$\bar{E}''(v) = \frac{E_d''(v) + x(v)E_a''(v)}{1 + x(v)}, \quad (13)$$

given that all derivatives $E_{a/d}^{(n)}$ with $n \geq 3$ can be ignored. By substitution of the v_i 's by Dunham expansions [26], finally, the full revival time of the coupled system can be expressed in terms of those of the diabatic and adiabatic states:

$$\frac{1}{T_{1/1}^{\text{rev}}} = \frac{f}{T_{1/1}^{\text{a,rev}}} + \frac{(1-f)}{T_{1/1}^{\text{d,rev}}}. \quad (14)$$

Equation (14) gives an excellent account of the observed revival times in full quantum dynamics calculations in both bound and predissociative systems [18]. From the semiclassical picture it follows that a general condition for the existence of bistable wave-packet motion is that there is a range of near-resonant diabatic and adiabatic vibrational levels. This requirement is, in principle, independent of the coupling and can be fulfilled for any coupling strength.

III. MODEL SYSTEM AND CALCULATIONS

The process of quantum wave-packet preparation and its subsequent evolution was here modeled within the framework of the system in Fig. 1. The three molecular electronic states have potential energy curves that are slightly shifted replicas of the three lowest states in the Rb_2 molecule. An ultrafast laser pulse couples the initially only populated ground state $|0\rangle$ to the excited state $|1\rangle$. The two excited states, in turn, are coupled to each other by some intramolecular mechanism, which in Rb_2 would be electronic spin-orbit interactions, mainly.

The quantum dynamics of the system was calculated by solving the time-dependent Schrödinger equation for the time-dependent total wave function $\Psi(r, t) = \langle r | \Psi; t \rangle$,

$$i\hbar \partial_t \Psi(r, t) = H(r, t) \Psi(r, t), \quad (15)$$

via the split-operator method [27]. The three-state Hamiltonian was represented as

$$H(r, t) = \begin{bmatrix} T + V_{00}(r) & V_{01}(t) & 0 \\ V_{10}(t) & T + V_{11}(r) & V_{12}(r) \\ 0 & V_{21}(r) & T + V_{22}(r) \end{bmatrix}, \quad (16)$$

where $T = -(2\mu)^{-1} \hbar^2 \partial_r^2$ is the kinetic energy operator.

Employing the electric dipole and semiclassical approximations for the light-molecule interaction [28], we have $V_{01}(t) = V_{10}(t) = -\mu_{10} E(t)$, with μ_{10} being the transition dipole moment and $E(t)$ the classical electric field of the laser pulse. We took μ_{10} to be constant and $E(t)$ to have a Gaussian temporal profile $E(t) = E_0 \exp[-t^2/\Delta^2] \cos[\omega_0 t]$ with $\mu_{10} E_0 = 1 \times 10^{-4}$ a.u. and $\Delta = 3511.28$ a.u. These laser pulse values correspond to a 100-fs-long pulse with intensity and population transfer in the perturbative range.

The molecular potential energy curves were represented by Morse functions $V_{ii}(r) = D_i \{1 - \exp[-\alpha_i(r - r_i)]\}^2 + T_i$, with parameter values as specified in Table I. The intramolecular coupling between the two excited electronic states in the

TABLE I. Parameter values (in atomic units) for the Morse potential energy curves $V_{ii}(r) = D_i \{1 - \exp[-\alpha_i(r - r_i)]\}^2 + T_i$ of the model system.

$ i\rangle$	T_i	D_i	α_i	r_i
$ 0\rangle$	0.00000	0.01749	0.39397	6.7690
$ 1\rangle$	0.04853	0.02644	0.25727	8.8600
$ 2\rangle$	0.04311	0.03206	0.33763	7.6881

calculations was $V_{12}(r) = V_{21}(r) = A \exp[-\beta(r - r_\times)^2]$ with $A = 4.945\,454\,55$ a.u., $\beta = 0.5$ a.u., and $r_\times = 9.3187$ a.u.

The initial wave function $\Psi(r, t \rightarrow -\infty) \equiv \langle 0, r | \Psi; t \rightarrow -\infty \rangle$ was taken to be that of the vibrational ground state of $|0\rangle$ and was calculated by the Fourier grid Hamiltonian method [29]. The split-operator propagation was done on a grid of 4096 points covering the r range 4.0–24.0 a.u. During the laser pulse action, a propagation step of 0.413 41 a.u. (0.01 fs) was used and after that the propagation step was set to 41.341 a.u. For consistency with the choice of molecular potentials, the reduced molecular mass μ was chosen to be that of the rubidium molecule in natural isotope abundance, 77 899.1 a.u. (42.7339 amu).

The Morse potential energy curves correspond to the three lowest electronic states in Rb_2 , $X^1\Sigma_g^+$, $A^1\Sigma_u^+$, and $b^3\Pi_u$, and were obtained by fits to those calculated by Park *et al.* [30], $V_\alpha(r)$, $\alpha = X, A, b$. For the present calculations, the curves were shifted in r position as $V_{00}(r) = V_X(r - 0.9946$ a.u.), $V_{11}(r) = V_A(r - 0.1172$ a.u.), and $V_{22}(r) = V_b(r)$. These shifts can be thought of as mimicking the experimentally accessible processes of wavelength selection of the wave-packet launch position (ground-state shift) and rotational-state selection (excited-state relative shift) in a thermally excited molecular system. The relative excited state potential shift and other parameter adjustments were done such that a wave packet with a total energy of $E_{\text{bs}} = 0.062\,096$ a.u. starting at either one of the outer classical turning points of the excited states would undergo simple bistable mesobatic motion with full long-term revivals, similarly to what was first demonstrated in [18]. To obtain maximally mixed motion, moreover, the wave-packet splitting ratio at the potential curve crossing was arranged to be 50:50.

The laser pulse duration and Rabi cycling time were chosen to be significantly shorter than the characteristic vibrational period of the excited states. The main action of the pulse, thus, was to create a wave packet in the excited state $|1\rangle$, and in the following we will ignore all subsequent dynamics in $|0\rangle$ and renormalize the excited-state wave packet accordingly. Likewise, all expectation values, etc., are taken to refer to the subspace of the two excited electronic states only. To facilitate characterization of the (sub)system dynamics, we introduce the correlation functions

$$S_i^{\text{in/out}}(t) = \langle \Psi_i; t_i^{\text{in/out}} | \Psi_i; t \rangle, \quad (17)$$

where $|\Psi_i; t\rangle = \langle i | \Psi; t \rangle$. $t_i^{\text{in/out}}$ refers to the time of the first occurrence of the wave packet at, respectively, the inner and outer turning points of $V_{ii}(r)$. That is, $t_i^{\text{out}} \approx \langle T_{\text{cl}} \rangle / 2$ and $t_i^{\text{in}} \approx \langle T_{\text{cl}} \rangle$, where $\langle T_{\text{cl}} \rangle$ is the average classical vibrational period

of the adiabatic states, which is about 1 ps. In the case of t_i^{in} , the reference wave function was obtained after removal of the wave-packet fraction in $|1\rangle$ at $t=t_i^{\text{out}}$. The full set of $S_i^{\text{in/out}}(t)$, hence, measures the similarity of the wave packet to its more or less nascent form at the turning points of the potential curve of each electronic state. Their amplitudes are bounded by the instantaneous population in the respective states.

IV. RESULTS

The model system was designed such that the bistable interference condition (7) would be fulfilled for a wave packet starting at either outer turning point with a total energy of E_{bs} and that the initial wave-packet splitting ratio would be 50:50. Such a wave packet would exhibit exceedingly regular motion with collapse-revival dynamics with the full revival time $T_{1/1}^{\text{rev}}$ given by (14) [18]. Moreover, the wave packet would be locked into the initially prepared bistable state of motion and never reach the outer turning point of the complementary one.

The dynamics becomes considerably more involved when the initial state instead is chosen to be one of the inner turning points. Such motion was found to be the origin of the short-term vibration dynamics in the $\text{Rb}_2(A \sim b)$ system [13–15], and our aim here is to gain further insight into the basic characteristics of this type of motion and its preparation by pulsed laser excitation. For this purpose, we begin by discussing the dynamics of a wave packet excited to the inner turning point of $|1\rangle$, as indicated in Fig. 1, with a total energy E_{bs} . The wave-packet energy can be controlled by variation of the laser wavelength, which is explored in the second part of the section.

A. Bistable interference conditions

1. Short-term dynamics

For a laser pulse with frequency $\omega_0=0.06196$ a.u., the excited wave-packet total energy $\langle H \rangle = E_{\text{bs}}$. This implies that the bistable interference condition (7) is fulfilled and results in the early dynamics reflected in the correlation functions shown in Fig. 3. Expectedly, the preparation of the wave packet in $|1\rangle$ is the first thing that happens. The low correlation value for the initial peak, it should be noted, is a consequence of our choice of reference function in (17). It does not reflect directly the population in $|1\rangle$, which was renormalized right after the excitation pulse had ended such that $N_1(t \approx \frac{\tau}{2}) = 1$. At its first encounter of the curve crossing, the wave packet splits in two fractions. These appear at the respective outer turning points at about $\langle T_{\text{cl}} \rangle / 2$ with equal squared correlation amplitudes of 0.25. By definition, the squared amplitude at this time corresponds to $[N_i(t_i^{\text{out}})]^2$ and thus shows that the wave packet has been split into halves. The wave-packet part in $|2\rangle$ is the one that first returns to the curve crossing and splits there into two quarter fractions of the initial wave function. It is shortly followed by the remaining fraction, which splits similarly. Hence, there are two closely spaced wave packets that copropagate towards each

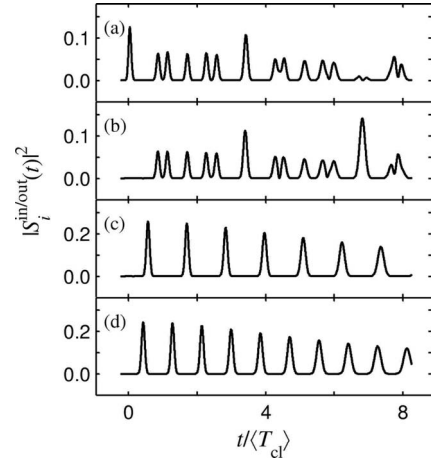


FIG. 3. Early-time dependence of the correlation function (17) at the turning points: (a) $|1\rangle$ inner, (b) $|2\rangle$ inner, (c) $|1\rangle$ outer, and (d) $|2\rangle$ outer.

inner turning point, as can be seen in the two upper panels of Fig. 3.

The system has been set up to fulfill the bistable interference conditions for a wave packet evolving from either of the outer turning points. Consequently, the two wave-packet fractions originating from the outer turning point in $|2\rangle$ arrive simultaneously at the curve crossing and recombine such that the resulting wave packet goes completely back into $|2\rangle$. This is seen as the second peak in Fig. 3(d), which, accordingly, has the same amplitude as the first one. Meanwhile, the wave-packet fraction originating from the other outer turning point recombines and follows the complementary bistable motion back to the outer turning point of $|1\rangle$; see Fig. 3(c).

The difference in classical vibrational periods for the two bistable states motion is readily seen in the two bottom traces of Fig. 3. This difference leads to an increasingly complex pattern of overlapping wave-packet fractions at the inner turning points. The evolution of the correlation functions at the other end points of the motion, however, remains very regular and has in each case the appearance of simple bistable motion. The decrease in amplitudes in that case is caused by spreading of each wave-packet fraction.

2. Long-term dynamics

On a time scale exceeding a few vibrational periods, the initially well-localized wave-packet parts spread and start to overlap and, in general, the correlation functions become erratically fluctuating. This is in Fig. 4 shown to be the case for the correlation functions at the inner turning points. The corresponding measures at the outer turning points, however, exhibit remarkable regularities. In fact, they look precisely like fractional and full revival structures in autocorrelation traces for wave packets moving in single anharmonic potentials [25] or, as we recently showed [18], in a coupled system under bistable mesobatic conditions similar to the present case. The squared correlation amplitude of 0.25 at the outer turning points at around $t=200\langle T_{\text{cl}} \rangle$ and $400\langle T_{\text{cl}} \rangle$ indicates that the wave-packet fraction is identical to the nascent one, bar a possible complex factor with unity absolute value. This

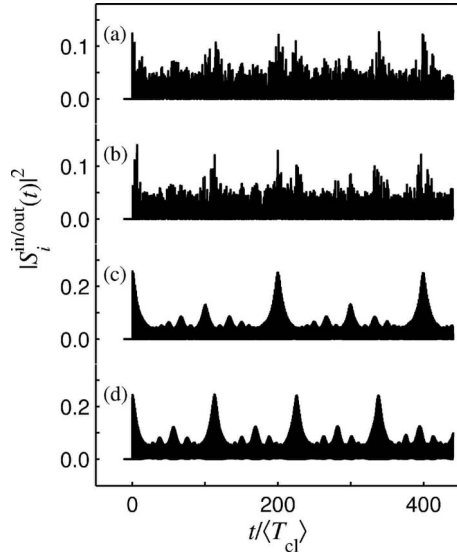


FIG. 4. Long-term evolution of the correlation function (17) at the turning points: (a) $|1\rangle$ inner, (b) $|2\rangle$ inner, (c) $|1\rangle$ outer, and (d) $|2\rangle$ outer.

means that, apparently, the wave-packet fraction has been revived. Consequently, the signal for this system will be very different depending on where the dynamics is probed. If the system is probed at the outer turning points of the excited states, regular signals are obtained, for both short and long time scales, whereas at the inner turning points they would appear as quite irregular except for the very first few vibrational periods.

To take the analysis one step further, we compare the apparent revival times of the wave-packet fractions to the predictions for bistable revival periods from application of (14). As seen in Fig. 5, the predicted revival times match exceedingly well those of the wave-packet fractions in the present system—the relative error [18] is on the order of 1%. This indicates that the full wave-packet dynamics in Fig. 4 actually may be viewed as being composed of two independent wave packets undergoing separate bistable motion. This conjecture is corroborated by the exceptional similarity of the full wave-packet dynamics in Figs. 5(a) and 5(b) to those of the respective unperturbed bistable wave packets in Figs. 5(c) and 5(d). Here, each individual bistable wave-packet fraction was extracted from the full wave packet by quenching the part in the other electronic state at the first encounter of the outer turning points at $t \approx \langle T_{cl} \rangle / 2$. It is clearly seen that not only the revival times, but also the envelopes of the correlation functions of the single bistable wave packets are close to identical to the corresponding ones of the full wave packet.

The Wigner transform [31] can be used to bring further insight of the quantum dynamics. For the wave function $\psi_j(r) = \langle j, r | \Psi; t \rangle$, it is defined as

$$\mathcal{W}_j(r, p) = \frac{1}{\pi\hbar} \int_{-\infty}^{\infty} ds e^{2ips/\hbar} \psi_j^*(r+s) \psi_j(r-s), \quad (18)$$

where p is the momentum. The corresponding phase-space distribution at the instant of the full revival of the wave-

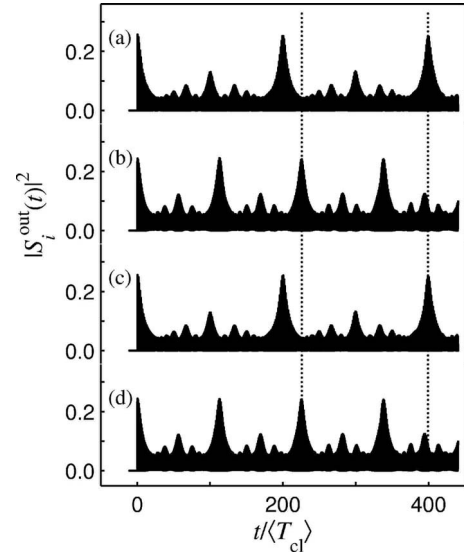


FIG. 5. Long-term evolution of the correlation function (17) at the outer turning points for the whole wave packet as well as for the fraction remaining after depleting the wave-packet part in the complementary state at $t \approx \langle T_{cl} \rangle / 2$. (a) $i=1$, full wave packet. (b) $i=2$, full wave packet. (c) $i=1$, wave-packet part in $|2\rangle$ depleted at $t \approx \langle T_{cl} \rangle / 2$. (d) $i=2$, wave-packet part in $|1\rangle$ depleted at $t \approx \langle T_{cl} \rangle / 2$. The full revival times of the initial two wave-packet fractions in unperturbed bistable mesobatic motion (14) are indicated by vertical dashed lines.

packet fraction in $|2\rangle$ is shown in Fig. 6. The revived well-localized wave-packet fraction is clearly seen in part (a) at the outer turning point of $|2\rangle$, while the remaining wave-packet part is spread out all over $|1\rangle$ and the inner part of $|2\rangle$. About half a vibrational period later, we find that the wave-packet fraction previously at the outer turning point of $|2\rangle$ has split into two well-localized fractions of equal amplitudes that are superimposed on the collapsed part of the wave function. It is clear from the ensuing evolution of $S_2^{\text{out}}(t)$ that the two localised wave-packet fractions recom-

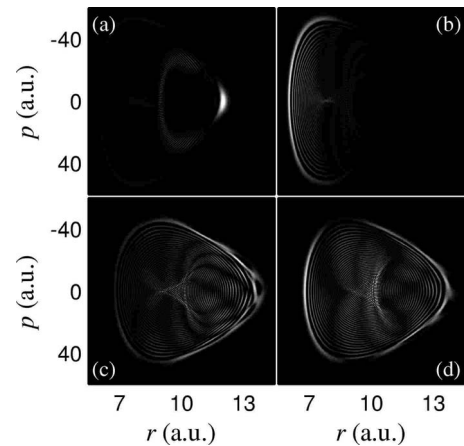


FIG. 6. Wigner transforms $W_i(r, p)$ of the system at times around $400\langle T_{cl} \rangle$. In (a) and (c) at the peak value of $S_2^{\text{out}}(t)$; (b) and (d) about $\langle T_{cl} \rangle / 2$ later. The graphs (a) and (b) refer to state $|2\rangle$ whereas (c) and (d) relate to $|1\rangle$. Only positive values of $W_i(r, p)$ are shown.

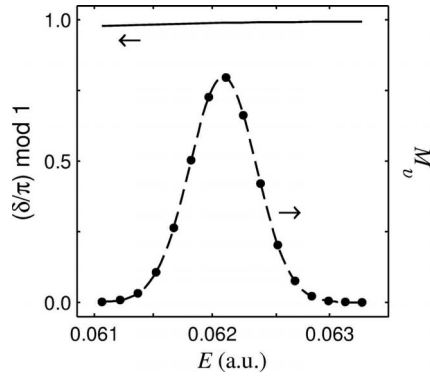


FIG. 7. Energy distribution of the wave packet in terms of Franck-Condon factors for projection onto the vibrational eigenstates of $|1\rangle$ (solid circles connected by the dashed line), $M_v = |\langle 1, v | \Psi; t \approx \tau/2 \rangle|^2$, together with the semiclassical phase difference $(\delta/\pi) \bmod 1$ (solid line), which should be close to either 0 or 1 for bistable interference conditions. Here, the value varies across the energy distribution of the wave packet from 0.98 to 0.99 and corresponds to $m=19$ in the bistable interference condition (7). The two ordinate scales are the same.

bine and go completely into state $|2\rangle$ as they reencounter the potential curve crossing. Thus, the motion for this wave-packet fraction at its full revival time is analogous to that during the very first few vibrational periods. The same applies for the other fraction at its time of revival.

Long-term stability of bistable mesobatic motion, as indicated in Sec. II C, would in the semiclassical picture be expected to entail that the interference condition (7) is fulfilled over the entire wave-packet energy range. The energy distribution of the wave packet is in Fig. 7 represented by the population projection of the wave packet onto the vibrational eigenstates of the electronic state $|1\rangle$ right after the excitation pulse has ended, $M_v = |\langle 1, v | \Psi; t \approx \tau/2 \rangle|^2$. Indeed, the semiclassical phase difference δ also plotted in Fig. 7 is very close to an integer multiple of π and it is so over the whole energy range covered by the excited wave packet.

B. Excitation wavelength variation

A wave packet excited to a total energy $E_{bs} = 0.062096$ a.u. under the present initial conditions splits in two equally large parts that undergo individual regular bistable motion. This was achieved by choosing the frequency of the exciting laser pulse ($\omega_0 = 0.06196$ a.u.) such that the resulting excited part of the wave packet had an energy E_{bs} at which the semiclassical phase difference δ was equal to an integer times π . In general, a small change in the energy of the wave packet from E_{bs} breaks the interference condition and causes for small deviations reduced regularity in the long-term dynamics. Larger energy variations lead to qualitatively different dynamics. The wave-packet energy principally is governed by the carrier frequency ω_0 of the excitation pulse. This opens a route to selective preparation of bistable motion, in general, and the above-observed double bistable state of motion, in particular, by variation of the exciting laser wavelength.

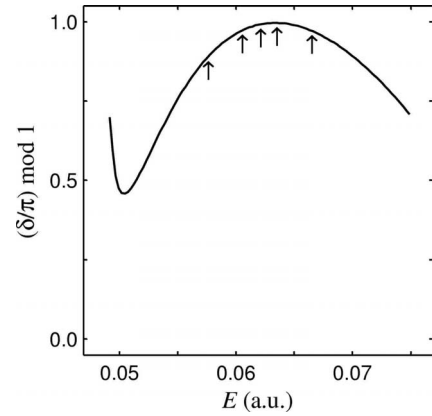


FIG. 8. The same semiclassical phase difference $(\delta/\pi) \bmod 1$ as in Fig. 7 over a wider energy range. The total wave-packet energies selected for calculation of the long-term correlation functions in Fig. 9 are indicated by arrows.

The semiclassical phase difference δ for a wave packet energy of E_{bs} in the present system is very nearly an integer multiple of π over the whole energy range covered by the wave packet. On a larger energy scale (see Fig. 8), δ changes significantly. Hence, we would expect the longterm regularity of the bistable motion to deteriorate if ω_0 is varied. This is also what is seen when we compare in Fig. 9 the evolution of $S_2^{\text{out}}(t)$ for the selected wave-packet energies marked in Fig. 8. The middle panel of Fig. 9 is the same as Fig. 4(c) and thus represents the bistable case discussed above. The well-developed full revival structure under those conditions is still visible, but severely distorted for the two energies closest to E_{bs} , whereas there is no sign of revivals for the two energies farther away from E_{bs} . Another observation is that not only the magnitude of δ is of importance. The two correlation functions with the nonoptimal energies $E = 0.060550$ a.u. and $E = 0.063520$ a.u. have about the same δ , but nevertheless, one is more regular than the other. The

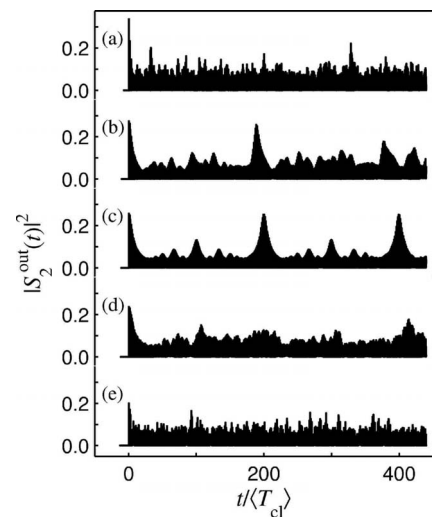


FIG. 9. The long-term evolution of $S_2^{\text{out}}(t)$ for wave packets excited to the total energies indicated in Fig. 8. From the bottom up $E = 0.057606$, 0.060555 , 0.062096 (E_{bs}), 0.063520 , 0.066495 a.u. The middle panel is the same as Fig. 4(c).

slope of δ versus E is quite different in the two cases, however. Thus, the difference in long-term stability for these two energies in a sense illustrates the importance of the semiclassical requirement that the interference condition should be fulfilled over the whole wave-packet energy range.

V. DISCUSSION

The calculations presented above show that it is in a suitable molecular system would be feasible to prepare bistable mesobatic wave-packet states—strongly mixed hybrid diabatic-adiabatic states of motion [13,14] with highly regular long-term dynamics [18]—in accordance with the previous interpretation of ultrafast pump-probe experiments on predissociative [10–12] and bound [13–15] diatomic molecular systems. Such motion in molecules represents a severe breakdown of the Born-Oppenheimer approximation, and neither a diabatic nor an adiabatic picture provides a convenient representation of the system dynamics. The present model system was arranged such as to facilitate investigation of principal properties of the preparation and evolution that could be expected of such wave-packet states. Accordingly, we will in this section discuss particular aspects of bistable-state preparation and identification and the fundamental coupled-system dynamics.

The preparation of a wave packet in a bistable state of motion, obviously, requires that the coupled system feature the appropriate interference condition (7) for some energy. If, in addition, one of the corresponding electronic states is accessible from the electronic ground state at the required internuclear separation, then the whole matter of state preparation reduces to simple laser wavelength tuning, as shown in Sec. IV B. The semiclassical analysis of the phase difference δ might be used to identify suitable systems fulfilling these conditions. Thermal excitation might be influential both by modifying the phase difference δ by means of the rotational-state dependence of the effective potential surfaces and couplings and by widening of the accessible range of internuclear separation for the wave-packet launch by vibrational excitation of the electronic ground state.

The wave-packet dynamics after launch into a bound system under bistable interference conditions could involve simple bistable motion only or, as shown here, initial wave-packet splitting and subsequent independent bistable evolution of two complementary wave-packet fractions. The point of wave-packet launch decides which will be the prevailing situation. This, implicitly, is shown by Fig. 5, where each reference wave packet (b) and (d) mimics a situation in which the wave packet is launched at the outer turning point of one electronic state. These wave packets undergo simple bistable motion and never reach the outer turning point of the opposite electronic states. A wave packet launched at an inner turning point, on the other hand, first splits into two fractions. As argued below, these two fractions then evolve each in a bistable motion like the other fraction was absent. A bound system featuring bistable interference conditions, thus, supports two basic types of mesobatic wave-packet dynamics, simple bistable motion and a bistable twin state of motion comprising independent bistable evolution of two

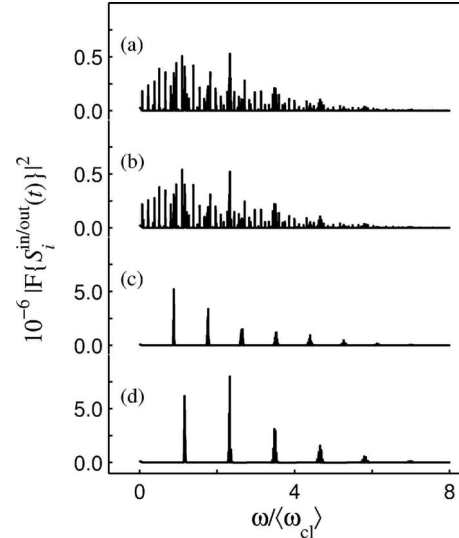


FIG. 10. Power spectra versus frequency ω , in terms of the average vibrational frequency $\langle\omega_{cl}\rangle = \langle T_{cl}\rangle^{-1}$, of the long-term correlation functions at the various turning points in Fig. 4: (a) |1> inner, (b) |2> inner, (c) |1> outer, and (d) |2> outer. $F\{\cdot\cdot\}$ denotes the Fourier transform.

wave-packet fractions created by splitting of the launched wave packet at its first passage of the potential curve crossing. A predissociating system, in contrast, can only support the simple type of bistable motion, as it does not provide more than one simple bistable state of mesobatic motion.

The simple type of bistable mesobatic motion was observed in experiments on predissociation of IBr molecules [10,11], while the split bistable wave-packet motion was seen to occur in bound-state dynamics in Rb_2 [13–15]. In both experiments a pump-probe scheme was used, which is a frequently employed work horse in ultrafast molecular spectroscopy. It is a conceptually very simple method in that a dynamical process is initiated with an ultrashort pump pulse and the ensuing system evolution is followed in time by a variably delayed ultrashort probe pulse. Implicitly, however, the outcome of such measurements depends critically on the choice of probe transition and the present bound model system provides a very clear illustration of this. Our correlation functions $S_i^{\text{in/out}}(t)$, namely, resemble very much what would be obtained by suitably tuned probe pulses. Thus, depending on the choice of the side of the potential curve crossing to be probed, the observed long-term wave-packet dynamics would appear regular or irregular, similar to what can be seen in Fig. 4. This is also evident in the corresponding frequency spectra in Fig. 10. For the correlation functions at the outer turning points, accordingly, the spectra are very simple and only exhibit the vibrational frequency of the involved diabatic state and overtones of that, whereas the spectra for the inner turning points show no clear regularity at all. From another viewpoint, probing at one of the outer turning points—which may well be the only available option in an experiment—the observed regular signal would very easily be completely mistaken for simple vibrational motion in a single diabatic or adiabatic potential. In fact, not even the revival structures would give an obvious hint that the true

state of motion is a fully mixed diabatic-adiabatic one. Even if the latter circumstance would be clear, essential parts of the system dynamics could be missing in the signal, as another wave-packet fraction in the complementary bistable state of motion effectively would be invisible.

We recently have shown by numerical quantum dynamics calculations that wave packets in bistable states of mesobatic motion may exhibit long-term collapse-revival dynamics [18]. These states of simple motion come in complementary pairs, in accordance with the semiclassical theory reviewed in Sec. II B. Likewise, the semiclassical revival time (14) is in excellent agreement with that obtained from full quantum dynamics calculations [18]. The situation in the present system is more involved as it is an instance of the bistable twin state of motion. Accordingly, the early dynamics comprises splitting of the laser-excited wave packet at the first passage of the potential curve crossing. Each of the two wave-packet fractions then for a few vibrational periods undergoes recognizable bistable mesobatic motion that is rapidly obscured by interference between the various wave-packet parts. From Figs. 4–6, however, we see that each bistable wave-packet fraction is revived at its outer turning point at the time expected for a simple bistable system. Moreover, the fractional revival pattern in the correlation amplitudes $S_i^{\text{in/out}}(t)$ is similar to the autocorrelation patterns in the cases with single bistable wave packets. We thus see that the two wave-packet fractions that were split apart at the first curve crossing are locked into individual bistable mesobatic motion and that the subsequent dynamics of one fraction is not the least affected by the presence of the other wave-packet part, despite the fact that they share the same phase space and overlap in most of it. Otherwise, the revival time of each twin in the composite bistable wave-packet motion would not be that of the corresponding simple bistable motion. Another manifestation of this situation is that one of the bistable wave-packet fractions can be depleted without noticeable effect on the other part, as demonstrated in Fig. 5.

The splitting into two independent bistable wave-packet motions can be viewed as a direct consequence of the fundamental property of simple bistable wave-packet motion that the available phase space is restricted and different for the two bistable twin states. After the first traversal of the curve crossing, namely, the wave packet has been split into two orthogonal components: $|\Psi; \langle T_{\text{cl}} \rangle / 2 \rangle = c_1 |\Psi_1; \langle T_{\text{cl}} \rangle / 2 \rangle + c_2 |\Psi_2; \langle T_{\text{cl}} \rangle / 2 \rangle$, where the expansion coefficients obey $|c_1|^2 + |c_2|^2 = 1$. The orthogonality of these wave-packet fractions follows from the fact that they are located entirely in different parts of the phase space. The unitarity of the time evolution operator $U(t, t_0)$ then ensures that these components remain orthogonal for all t and that c_1 and c_2 are constants—that is,

$$|\Psi; t \rangle = c_1 |\Psi_1; t \rangle + c_2 |\Psi_2; t \rangle, \quad (19)$$

where $|\Psi; t \rangle = U(t, \langle T_{\text{cl}} \rangle / 2) |\Psi; \langle T_{\text{cl}} \rangle / 2 \rangle$ and similarly for the components. Clearly, the dynamics comprises two wave-packet fractions that evolve without mixing. Each of these by preparation is in a state of simple bistable motion, which means that $\langle \Psi_i; \langle T_{\text{cl}} \rangle / 2 | \Psi_j; t \rangle = 0$ for $i \neq j$. In other words, the imposed dynamical quantum interference prevents the wave-

packet fraction that starts out in one of the two initial states from developing amplitude in the phase-space region defining the other state. The close similarity in Fig. 5 between the correlation functions calculated at the outer turning points for the full and reduced wave packets, for which one of the initial components has been removed, thus is to be expected under bistable interference conditions. If these conditions would be relaxed, however, then there would be leakage of amplitude into the phase space of the complementary initial state and the result would be quite different, despite the fact that there is still no mixing of the orthogonal components of the full wave packet.

VI. CONCLUSION

We have seen here that a molecular wave packet created by an ultrashort laser pulse in a system of two coupled bound molecular states under suitable dynamical quantum interference conditions is split into two separable fractions. The two parts move in different but partially overlapping parts of the energetically available phase space. The wave-packet components, thus, can be identified and addressed individually in their unique section of molecular phase space. By these means it is readily seen that each wave-packet fraction evolves exactly like the other part were not there; that is, they go through long-term collapse-revival cycles analogous to those of wave packets moving in single anharmonic potentials [18] and the depletion of one wave-packet component does not affect the other.

The choice of molecular configuration to probe—e.g., in an ultrafast pump-probe experiment—has under these conditions a great influence on the appearance of the dynamics. The regular, but different, collapse-revival dynamics observable in the separated parts of the phase space takes on a quite irregular appearance in the regions that are shared by the wave-packet components. The wave-packet regularity was shown to depend sensitively on the pump pulse wavelength, which is a reflection of the energy range over which the quantum interference conditions are maintained. These conditions, as well as the wave-packet fraction revival times, are well reproduced by semiclassical theory, which appears to be a valuable tool for the identification and design of systems of the present kind.

The problem was here set in a molecular context, but the results are in no fundamental way restricted to such systems. Rather, we expect that the realization of the implied quantum control scheme may be more easily achieved in other physical systems. Nonetheless, recent theoretical work [32–35] indicates that there may be practically achievable ways of manipulating molecular systems that are known to exhibit clear traits of the here-discussed type of wave-packet motion [11,13–15].

ACKNOWLEDGMENTS

We thank Jonas Larson for much valuable discussions. This work was supported by the Swedish Research Council (VR).

- [1] S. A. Rice, *Nature (London)* **409**, 422 (2001).
- [2] M. Shapiro and P. Brumer, *Principles of the Quantum Control of Molecular Processes* (Wiley, Hoboken, NJ, 2003).
- [3] A. Einstein, *Sitzungsber. Preuss. Akad. Wiss., Phys. Math. Kl.* **1925**, 3.
- [4] E. C. G. Stückelberg, *Helv. Phys. Acta* **5**, 369 (1932).
- [5] M. S. Child, *Mol. Phys.* **32**, 1495 (1976).
- [6] T. S. Rose, M. J. Rosker, and A. H. Zewail, *J. Chem. Phys.* **91**, 7415 (1989).
- [7] H. Kono and Y. Fujimura, *Chem. Phys. Lett.* **184**, 497 (1991).
- [8] S. Chapman and M. S. Child, *J. Phys. Chem.* **95**, 578 (1991).
- [9] C. Meier, V. Engel, and J. S. Briggs, *J. Chem. Phys.* **95**, 7337 (1991).
- [10] M. J. J. Vrakking, D. M. Villeneuve, and A. Stolow, *J. Chem. Phys.* **105**, 5647 (1996).
- [11] M. Shapiro, M. J. J. Vrakking, and A. Stolow, *J. Chem. Phys.* **110**, 2465 (1999).
- [12] A. N. Hussain and G. Roberts, *J. Chem. Phys.* **110**, 2474 (1999).
- [13] B. Zhang, N. Gador, and T. Hansson, *Phys. Rev. Lett.* **91**, 173006 (2003).
- [14] N. Gador, B. Zhang, H. O. Karlsson, and T. Hansson, *Phys. Rev. A* **70**, 033418 (2004).
- [15] N. Gador, B. Zhang, and T. Hansson, *Chem. Phys. Lett.* **412**, 386 (2005).
- [16] D. Wang, T. Hansson, Å. Larson, H. O. Karlsson, and J. Larson, *Phys. Rev. A* **77**, 053808 (2008).
- [17] H. Dietz and V. Engel, *Chem. Phys. Lett.* **255**, 258 (1996).
- [18] D. Wang, Å. Larson, H. O. Karlsson, and T. Hansson, *Chem. Phys. Lett.* **449**, 266 (2007).
- [19] M. S. Child, *Semiclassical Mechanics with Molecular Applications* (Clarendon Press, Oxford, 1991).
- [20] L. D. Landau, *Phys. Z. Sowjetunion* **2**, 46 (1932).
- [21] C. Zener, *Proc. R. Soc. London, Ser. A* **137**, 696 (1932).
- [22] G. Wentzel, *Z. Phys.* **38**, 518 (1926).
- [23] H. A. Kramers, *Z. Phys.* **39**, 828 (1926).
- [24] L. Brioullin, *Compt. Rend.* **24**, 183 (1926).
- [25] R. W. Robinett, *Phys. Rep.* **392**, 1 (2004).
- [26] C. H. Townes and A. L. Schawlow, *Microwave Spectroscopy* (Dover, New York, 1975), Chap. 1.
- [27] M. D. Feit, J. J. A. Fleck, and A. Steiger, *J. Comput. Phys.* **47**, 412 (1982).
- [28] R. Loudon, *The Quantum Theory Of Light*, 2nd ed. (Clarendon Press, Oxford, 1983).
- [29] C. C. Marston and G. G. Balint-Kurti, *J. Chem. Phys.* **91**, 3571 (1989).
- [30] S. J. Park, S. W. Suh, Y. S. Lee, and G.-H. Jeung, *J. Mol. Spectrosc.* **207**, 129 (2001).
- [31] M. Hillery, R. F. O'Connell, M. O. Scully, and E. P. Wigner, *Phys. Rep.* **106**, 121 (1984).
- [32] B. J. Sussman, D. Townsend, M. Y. Ivanov, and A. Stolow, *Science* **314**, 278 (2006).
- [33] J. González-Vázquez, I. R. Sola, J. Santamaria, and V. S. Malinovsky, *Chem. Phys. Lett.* **431**, 231 (2006).
- [34] J. González-Vázquez, I. R. Sola, J. Santamaria, and V. S. Malinovsky, *J. Chem. Phys.* **125**, 124315 (2006).
- [35] J. González-Vázquez, I. R. Sola, J. Santamaria, and V. S. Malinovsky, *J. Phys. Chem.* **111**, 2670 (2007).